

Conceptualizing Uncertainty

Isaac Roberts, Alexander Schulz, Sarah Schröder, Fabian Hinder, and Barbara Hammer

Machine Learning Group, Bielefeld University, D-33619 Bielefeld, Germany
 {iroberts, aschulz, saschroeder, fhinder, bhammer}@techfak.uni-bielefeld.de

Abstract Uncertainty in machine learning refers to the degree of confidence or lack thereof in a model’s predictions. While uncertainty quantification methods exist, explanations of uncertainty, especially in high-dimensional settings, remain an open challenge. Existing work focuses on feature attribution approaches which are restricted to local explanations. Understanding uncertainty, its origins, and characteristics on a global scale is crucial for enhancing interpretability and trust in a model’s predictions. In this work, we propose to explain the uncertainty in high-dimensional data classification settings by means of concept activation vectors which give rise to local and global explanations of uncertainty. We demonstrate the utility of the generated explanations by leveraging them to refine and improve our model.¹

Keywords: Explainable Uncertainty· Concept-based Explanations· XAI.

1 Introduction

While advances in deep learning in the last years have led to impressive performance in many domains, such models are not always reliable, particularly when it comes to generalizing to new environments or adversarial attacks. To improve on that, numerous methods have been developed in the field of explainable artificial intelligence (xAI) [5] to provide insights into model behavior and facilitate actionable modifications. However, the majority of methods focus on explaining model *predictions*, which can help understand misclassifications but do not explicitly address predictive *uncertainty* (See Figure 1). Understanding uncertainty is crucial for detecting potential model weaknesses, particularly in dynamic environments.

Since uncertainty quantification is useful in various applications, including active learning [20], classification with rejects [17], adversarial example detection [26], and reinforcement learning [24], a significant body of work aims to improve the quantification of predictive uncertainty using Bayesian deep learning (BDL) and approximations thereof [15,9,14]. In contrast, the literature on understanding the sources of uncertainty for a given model via explanations is limited, focusing on methods for feature attribution [28,27] (see section 2.4 for more related

¹ Code will be freely available here (upon acceptance): <https://github.com/roberts120/Conceptualizing-Uncertainty>.

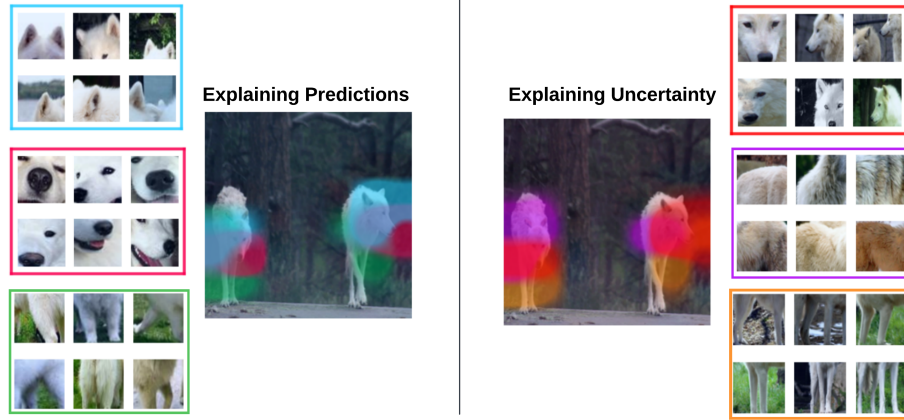


Figure 1: A White Wolf classified as Samoyed by an ImageWoof-adapted ResNet50 classifier. We generated the concept attribution map explaining the prediction (**left**) versus explaining the uncertainty (**right**) with our proposed pipeline. Correspondingly, we display three important concepts for this image using each explanation approach. The prediction explanation suggests the neural net arrived at its decision due to the detected concepts of a Samoyed’s ears, face, and legs, while the uncertainty explanation offers that the model is uncertain about its prediction because of the detected concept of a wolf’s head, fur, and legs.

work). While these approaches do provide valuable insights for individual input data points, they are restricted to local explanations and do not provide high-level insights on a global dataset scale, e.g., for image datasets. Also, another limitation of feature attribution methods, known from the prediction attribution setting and prevalent in the image domain, is that these point to *which* part of the input the model considers as important, but not *why* [13]. Here, methods aiming to automatically extract concept activation vectors (CAVs) [11,1] and attributing them back to the input do provide both, information on what the model seems to perceive in a part of the input, and global dataset information, both by inspecting the learned concepts.

In this work, (i) we propose a pipeline to enable concept-based explanations for predictive uncertainty, providing both local and global explanations for sources of uncertainty, and (ii) we demonstrate the correctness and usefulness of the learned concepts as well as the potential to perform actionable interventions based on these in a series of downstream tasks, including the automatic detection of different types of novelty in new environments, improving uncertainty-based rejections and detecting gender bias in language models.

We proceed by describing foundations for our contributions, including related work on uncertainty explanations. This is followed by our proposed pipeline in section 3, experiments in 4, a discussion on limitations in 5 and a conclusion.

2 Background

In this section, we list the relevant fundamentals, including our problem formulation, background on uncertainty quantification and concept activation vectors, as well as related work on explaining uncertainty.

2.1 Setup and Problem Formulation

Given a trained classification model \mathbf{M} , e.g., a deep convolutional network, and a dataset of n data points $\mathbf{X} = \{\mathbf{x}_1, \dots, \mathbf{x}_n\}$, usually not seen during training. In contrast to a vast amount of literature focusing on explaining predictions of such models [5], we aim for explaining their predictive uncertainty, thereby aiming to understand its sources. Our work differs from existing recent research on that topic, e.g., [5], in that we aim for global explanations.

For the following Bayesian formalization, we also require the training data set \mathcal{D} of \mathbf{M} , which, however, is not used by our method.

2.2 Quantifying Uncertainty

Predictive uncertainty is typically defined over the predictive distribution $p(y|\mathbf{x}, \mathcal{D})$ [15,9], which in our case is over possible labels y . In a Bayesian setting, where the parameters $\boldsymbol{\theta}$ of our classification model \mathbf{M} are random variables, $p(y|\mathbf{x}, \mathcal{D}) = \mathbb{E}_{p(\boldsymbol{\theta}|\mathcal{D})}[p(y|\mathbf{x}, \boldsymbol{\theta})]$ requires computing the expectation \mathbb{E} over the posterior $p(\boldsymbol{\theta}|\mathcal{D})$, which in practice is usually intractable. Accordingly, various methods for posterior approximation have been introduced such as ensemble methods [21], Monte Carlo (MC) dropout [14] and Laplace Approximations [6].

Different measures for predictive uncertainty are defined in literature [15,9]. We summarize the ones we are using in our experiments in the following.

Total Uncertainty based on Shannon Entropy:

$$u_t(\mathbf{x}) := \mathcal{H}[p(y|\mathbf{x}, \mathcal{D})] = - \sum_{y \in Y} p(y|\mathbf{x}, \mathcal{D}) \log_2 p(y|\mathbf{x}, \mathcal{D}) \quad (1)$$

Aleatoric and Epistemic Uncertainty based on the decomposition of u_t :

$$u_a(\mathbf{x}) := \mathbb{E}_{p(\boldsymbol{\theta}|\mathcal{D})}[\mathcal{H}[p(y|\mathbf{x}, \boldsymbol{\theta})]], \quad u_e(\mathbf{x}) := u_t(\mathbf{x}) - u_a(\mathbf{x}) \quad (2)$$

In order to approximate the above measures, we utilize MC dropout to collect a set predictions $\{p(y|\mathbf{x}, \boldsymbol{\theta}_i)\}_{i=1}^N$ and approximate the posterior predictive $p(y|\mathbf{x}, \mathcal{D}) = \mathbb{E}_{p(\boldsymbol{\theta}|\mathcal{D})}[p(y|\mathbf{x}, \boldsymbol{\theta})] \approx \frac{1}{N} \sum_i^N p(y|\mathbf{x}, \boldsymbol{\theta}_i)$. We refer to $\hat{u}_t, \hat{u}_a, \hat{u}_e$ when utilizing this approximation in u_t, u_a, u_e , respectively.

2.3 Concept Activation Vectors

Concept Activation Vectors (CAVs) aim for human interpretability with respect to understanding black-box model predictions [19,11,16]. Recent approaches

based on Nonnegative Matrix Factorization (NMF) [13,18] have been shown to demonstrate superior qualitative and quantitative properties of the resulting concepts[11]. They work by embedding patches of inputs into a non-negative activation space of a pre-trained model and applying NMF to decompose the embedded data matrix \mathbf{A} into a product of non-negative matrices \mathbf{W} and \mathbf{V} , solved by reconstructing \mathbf{A} , i.e., $(\mathbf{W}, \mathbf{V}) = \arg \min_{\mathbf{W} \geq 0, \mathbf{V} \geq 0} \|\mathbf{A} - \mathbf{W}\mathbf{V}^\top\|_F^2$. The decomposition yields: \mathbf{V} the dictionary of concepts (or concept bank) and \mathbf{W} a reduced representation of \mathbf{A} according to the basis \mathbf{V} . To attribute importance, they make use of a sensitivity analysis technique known as total Sobol Indices, which captures the effects of a concept along with its interactions on the model's output by considering the variance fluctuations by perturbing \mathbf{W} .

2.4 Related Work on Explaining Uncertainty

While there does exist a plethora of xAI methods for explaining the prediction of classification models including several local and global approaches [5], methods for explaining the source of uncertainty have only developed in the last years. So far, these have focused on local feature attribution explanations, including explaining uncertainty with shapley values [28], with gradient-based methods [27], with counterfactuals [2] and by taking second order effects into account [4]. In contrast, we aim for explanations beyond feature attribution, that provide also global explanations of uncertainty, which enable an overview of characteristics of uncertain predictions. Also, concerning image datasets, rather small ones consisting of MNIST and CIFAR are used in [28,27,2]. Only [4] is applied to CelebA, containing larger images. We apply our approach to images of ImageNet.

Another, less related line of work, aims for uncertainty sets, dealing with the problem of uncertainty of explanations [22].

3 Proposed Pipeline

We propose to explain predictive uncertainty by means of CAVs computed on a local level – for each data point – or aggregated to obtain a global explanation. In Figure 2, we illustrate our proposed pipeline which aims to characterize and explain uncertainty using extracted concepts using high-dimensional data \mathcal{D} . Given also a classification model \mathbf{M} , and an uncertainty measure u , e.g., $u := \hat{u}_t$, we arrange our pipeline into 4 steps:

Step 1 - We use the model \mathbf{M} to classify the inputs and compute $u(\mathbf{x})$ for each data point, by leveraging an approximation technique such as MC Dropout.

Step 2 - To apply concept activations, we need to specify a probabilistic classification task. In our setup, a canonical choice is the grouping induced by uncertain (UNC) and certain (CER) samples. To obtain a reasonable decision boundary, we observe that u will map CER to small numbers and UNC to large numbers. We therefore expect that if applied to all data points, $\{u(\mathbf{x}_i)\}_{i=1}^n$ can be described by a mixture model with two components. For simplicity, we assume a Gaussian Mixture Model (GMM) with two components which we train on $\{u(\mathbf{x}_i)\}_{i=1}^n$. By

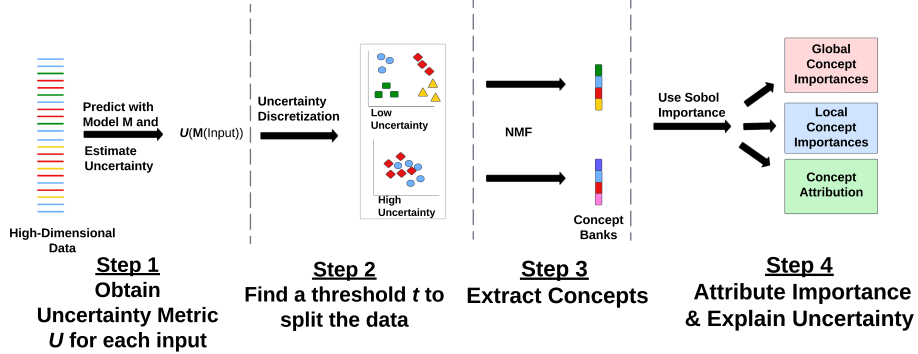


Figure 2: Our proposed pipeline for uncertainty explanation using CAVs.

our assumption we expect the component with the larger mean to correspond to the UNC samples. We thus obtain the classification model f by considering the conditional probability which takes on a sigmoid shape. To counteract potential class imbalance, i.e., an imbalance between CER and UNC in the training data, we set the weights of the mixture component to equal size after training.

Step 3 - To generate the concepts, we embed the data using a foundation model g into an activation space with the condition that for each \mathbf{x}_i , $g(\mathbf{x}_i) \geq 0$ (e.g., after a ReLU layer), and then we train one NMF on patches from $\{g(\mathbf{x}_i) | \mathbf{x}_i \in \text{UNC}\}$ and another NMF on patches from $\{g(\mathbf{x}_i) | \mathbf{x}_i \in \text{CER}\}$, producing two concept banks, \mathbf{V}_{UNC} and \mathbf{V}_{CER} . Thus, we can represent each $g(\mathbf{x}_i)$ as a linear combination of the concepts in \mathbf{V}_{UNC} or \mathbf{V}_{CER} , with scaling factors \mathbf{W}_i .

Step 4a - To estimate the importance of the concepts in \mathbf{V}_{UNC} and \mathbf{V}_{CER} , we utilize the Sobol Indices [12,13,18], using f as the function of interest.

Step 4b - Repeating Step 4a for every data point, we obtain a *local* importance score $e_l(g(\mathbf{x}_i)) \in \mathbb{R}^d$ with d concepts. Additionally, we supplement the local importances with an attribution map[13,18] indicating where the important concepts are detected in the input. We further augment the local explanations e_l with consistent global explanations. The *global* importances can be computed as in literature by averaging over $e_l(g(\mathbf{x}_i))$ for points predicted in UNC and CER, respectively, producing e_{UNC} and e_{CER} .

4 Experiments

Since uncertainty arises from multiple sources, establishing a ground truth for experimentation can be challenging. Therefore, we aim to demonstrate the validity and usefulness of our uncertainty explanations by integrating them into a classification with reject options setting. Additionally, we illustrate how our concepts capture different sources of uncertainty, aiding human decision-makers in constructing effective re-training sets. Finally, we show that our concepts can reveal potential biases with respect to sensitive groups in a downstream task.

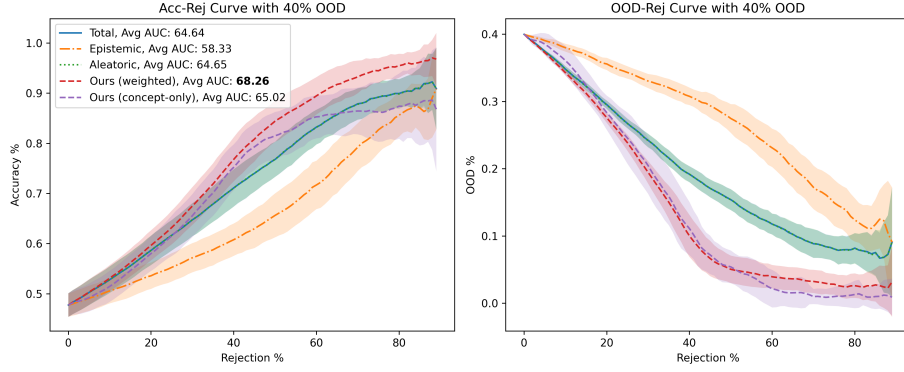


Figure 3: (left) Accuracy-Rejection (\uparrow) and (right) OOD-Rejection Curves (\downarrow).

4.1 Rejecting Uncertain Points with Concepts

We demonstrate that our proposed explanations enable actionable interpretations by utilizing the learned concepts for rejection decisions in a classification setting. In particular, given a trained model \mathbf{M} and a set of new data points \mathbf{X} , we apply our proposed approach to generate concept banks $\mathbf{V}_{\text{CER}}, \mathbf{V}_{\text{UNC}}$, according local importances $e_l(\mathbf{x}_i), \forall \mathbf{x}_i \in \mathbf{X}$ and global ones $e_{\text{CER}}, e_{\text{UNC}}$.

Now we consider the question: Can we improve a basic rejection strategy, which rejects a fixed amount of points based on predictive uncertainty, by leveraging our explanations? For the latter, we consider two strategies: 1. *Concept-only* rejection: we identify for each input \mathbf{x}_i the most strongly activated concept $c^* = \arg \max \mathbf{W}_i$ utilizing the combined concept bank $[\mathbf{V}_{\text{CER}}, \mathbf{V}_{\text{UNC}}]$ and determine the global importance of c^* . We then reject those points first, for which $c^* \in e_{\text{UNC}}$ and with highest e_{UNC} value. This leads to inputs associated with globally uncertain concepts being rejected first, while those linked to globally certain concepts being retained longer. 2. *Weighted* rejection: We adapt the previous strategy, by weighting the uncertainty output $f(\mathbf{x}_i)$ with $+1$ or -1 , depending on whether $c^* \in e_{\text{UNC}}$ or $c^* \in e_{\text{CER}}$ and again reject according to highest value.

To evaluate the effectiveness of these methods, we use a pre-trained ResNet-50 classifier as the base model. We randomly sample images from 10 out of 20 ImageNet classes (ImageWoof + Imagenette) and also include out-of-distribution (OOD) samples from the NINCO dataset [3]. In each run, we use 1,000 points, with 40% being OOD to compute accuracy-rejection curves [23,25], which depict the accuracy computed on all not-rejected points on the y-axis for different percentage rejection rates (x-axis). We compare our two concept-based strategies, Concept-only and Weighted rejects, to baselines, which reject according to highest predictive uncertainty, using each of $\hat{u}_t, \hat{u}_e, \hat{u}_a$. We also compute the AUC for each strategy and average these measures over 20 runs. We set the number of concepts to 55 for the certain group and 35 for the uncertain.

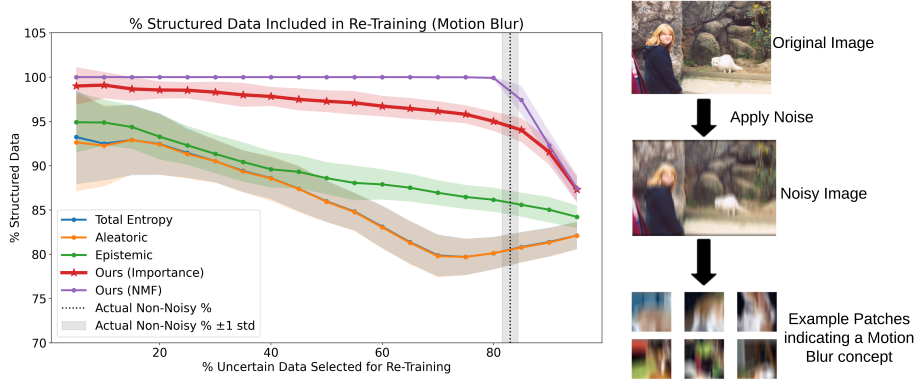


Figure 4: (left) Motion Blur experiment results (\uparrow) and an example noisy image (right) to better visualize the noise and the corresponding concept extracted.

As seen in Figure 3 (left), our "weighted" method performs with the highest AUC score computed across 20 runs. To confirm the statistical significance of this result, we conduct a one-sided Wilcoxon signed rank test against the Total Entropy (which in this case is very similar to the Aleatoric curve), obtaining a p -value $< 10^{-6}$, indicating ours performing significantly better. Meanwhile, the concept-only strategy performs better for medium rejection rates and worse for higher, as compared to the baselines.

In Figure 3 (right), we plot the percentage of OOD points among the not-rejected ones. Up to approximately 20% rejection, all curves except the Epistemic and Concept-only one, exhibit similar performance. However, beyond this point, both our strategies reject a greater proportion of OOD samples at each step. This signifies why our explanations improve the rejection: the learned concepts pick up on the OOD data and helps in rejecting them.

4.2 Distinguishing Sources for Uncertainty

In this experiment, we assess the quality and usefulness of the obtained explanations by showing that the learned concepts allow for a grouping of different sources of uncertainty, such that humans can better identify these sources and make more informed downstream decisions.

In particular, our setting involves a classifier \mathbf{M} that is applied in the wild and is exposed to two different types of noise. We consider structured noise induced by novel classes not seen during training and unstructured noise, like random distortions (e.g., blurring). We want to evaluate in how far our explanations can help to detect the different noise types and filter the instances with unstructured noise out, without having explicit knowledge about the noise beforehand. This can occur in an active learning setup, where a data exploration task could be to filter out unrecognizable noisy images that provide no meaningful learning signal and finetune the model on the remainder.

Table 1: We report the average AUC score (\uparrow) over 20 runs for various types of random noise patterns. Our methods using the local importances or reduced NMF representation perform better than the baselines. We test our methods against Gaussian Blurring (G Blur), Salt and Pepper Noise (S and P), Gaussian Noise (G Noise), Motion Blurring (M Blur), Radial Blurring (R Blur), and Wave Noise(Wave)

Method	Total	Aleatoric	Epistemic	Ours (Imp)	Ours (NMF)
G Blur	79.6 ± 1.5	79.5 ± 1.5	82.6 ± 1.2	85.6 ± 1.3	89.0 ± 0.2
SnP Noise	77.2 ± 1.4	77.3 ± 1.4	76.7 ± 1.7	85.4 ± 0.9	88.9 ± 0.2
G Noise	82.3 ± 1.3	82.5 ± 1.3	70.8 ± 2.7	85.1 ± 1.2	88.8 ± 0.3
M Blur	77.5 ± 2.0	77.4 ± 2.0	80.4 ± 1.4	87.0 ± 0.9	89.2 ± 0.2
R Blur	82.2 ± 1.6	82.4 ± 1.6	73.1 ± 2.9	85.2 ± 4.4	86.2 ± 4.9
Wave Noise	80.8 ± 7.4	80.1 ± 8.0	87.8 ± 2.0	88.3 ± 1.5	88.3 ± 1.5
Average	79.9 ± 2.2	79.9 ± 2.3	78.5 ± 6.3	86.1 ± 1.3	88.4 ± 1.1

More precisely, we consider the setting where new data samples \mathbf{X} are available and our explanation pipeline is applied to provide concept banks \mathbf{V}_{CER} , \mathbf{V}_{UNC} , according local importances $e_l(\mathbf{x}_i)$, $\forall \mathbf{x}_i \in \mathbf{X}$ and global ones e_{CER} , e_{UNC} . We aim to evaluate how well \mathbf{V}_{UNC} captures different noise types, and how well unstructured noise samples \mathbf{x}_i can be filtered out using $e_l(\mathbf{x}_i)$ and \mathbf{W}_i of \mathbf{V}_{UNC} concepts. For this purpose, we assume that we can determine the set nc that correspond to unstructured noise concepts in \mathbf{V}_{UNC} (as a human could visually inspect them). Then, for each data point \mathbf{x}_i , we sum the local importance $e_{l,nc}(\mathbf{x}_i)$ or NMF activations $\mathbf{W}_{i,nc}$ and filter out according to highest values, corresponding to the amount of presence of these concepts. We refer to these strategies as *Ours (Importance)* when using $e_{l,nc}(\mathbf{x}_i)$, and to *Ours (NMF)* for $\mathbf{W}_{i,nc}$.

To implement this experiment, we use a frozen and pre-trained ResNet50 bottleneck for g and train a classification head on ten dog species from the ImageWoof dataset, a subset of ImageNet [8]. We sample 1,000 images from the test set and introduce 150 out-of-distribution (OOD) images randomly selected from the NINCO dataset [3]. Additionally, we apply random noise to 10% of the ImageWoof images, according to one of {Gaussian noise, Salt and Pepper noise, Wave noise, Motion Blur, Gaussian Bur and Radial Blur}. We visually depict the effect of the Motion Blur in Figure 4 (right). For our pipeline, we utilize $u = \hat{u}_t$ and MC Dropout and consider baselines that rank data points according predictive uncertainty directly, filtering out first according to highest uncertainty. We utilize uncertainties based on $\hat{u}_t, \hat{u}_a, \hat{u}_e$. To simulate the human-in-the-loop that visually inspects \mathbf{V}_{UNC} , we utilize a linear logistic regression classifier trained on image patches in the NMF space to identify random noise. We record the percentage of informative data points for different percentages of data points kept from the uncertain set. The averaged curves over 20 iterations are plotted for Motion Blurring in Figure 4 and the according AUCs are summarized in Table 1.

The results in Table 1 indicate that our method outperforms uncertainty-based measures for this task. Thereby, using $e_l(g(\mathbf{x}_i))$ achieves the second-best performance (underlined), while leveraging \mathbf{W}_i yields the best results (bolded), with the highest average AUC score. Inspecting Figure 4, we can see that our method using the NMF coefficients (purple) consistently recommends images that would be beneficial to the re-training set while abstaining from recommending the unusable images until they must be chosen. We indicate the true unusable image percentage by the vertical line on the figure. In the ideal case, a method would not recommend any unusable images until it reaches the vertical line. Our method provides an explainable way to automatically select images which contain meaningful structure for domain adaptation.

4.3 Explaining Uncertainty in Language Models for Fairness

In this experiment, we demonstrate our proposed pipeline can also be applied to the natural language domain and that our explanations can capture sensitive group information, which can be used to correct bias in a model’s predictions.

For this purpose, we fine-tune a BERT [10] model on the Bias in Bios dataset [7] which consists of biographies where the task is to predict their corresponding occupation. Before fine-tuning, we incorporate ReLU on the last embedding layer to ensure non-negativity. We then apply our pipeline using a NMF-based concept extraction technique for the text domain [18]. We inspect the "physician" class, by training an NMF on the inputs predicted as such and compute their importances with respect to each group of uncertain and certain points.

We investigate the most important concept of the uncertain samples, number 6, in the following. In Figure 5, to understand what concept 6 represents, we show two excerpts which activate concept 6. Thereby, the intensity of red marks the strength of the activation of concept 6. We can see that female pronouns appear among the highlighted words along with other nouns like "co-founder" and "sleep medicine specialist". Since we know the gender labels of the dataset, we check the Pearson correlation between concept 6 and the labels. Indeed, it is the most correlated with gender at $R = 0.3$. We further verify the relevance of this concept for representing gender by excluding it in the NMF reconstruction and applying the occupation classifier. This changes some of the predictions, most notably a large proportion of professors and chiropractors that were falsely predicted as physicians. Even more interesting, the gender distribution among the samples influenced by concept 6 does not align with the gender distribution of said classes, which could be an indication of gender bias in BERT. We evaluate the change in gender bias by computing the equalized odd score before and after our intervention and report an improvement of 0.0027. At first glance this score does not sound impressive, the intervention on the physician class only affects a limited number of samples and thus has a limited effect on global equalized odds. More precisely, the best possible outcome for an intervention on the physician class (fixing all false positives) would have led to an improvement of 0.0069. This demonstrates that the detected relevant concept in the uncertain group encodes gender information in our example, and that removing it can improve fairness.

Her postgraduate work was completed in **the Child Health Associate/Physician Assistant Program** at the University of Colorado Health Sciences Center graduating in 2005

She has been working on a new app that **empowers** primary care, internal medicine **other practitioners** to deliver **great sleep care** throughout the medical system rather than just in the office of **a sleep medicine specialist**

Figure 5: Text excerpts where activations of concept 6 are highlighted with red.

5 Limitations and Future Work

While our approach performs well in the tasks outlined above, it is not without limitations. Concept-based explanations provide a human-interpretable means of understanding uncertainty in machine learning settings, particularly when the source of uncertainty is visibly discernible. However, they may fail to capture finer-grained pixel-level nuances of uncertainty. In this study, we maintained a fixed patch size when training the NMF, but varying the patch size could potentially capture more localized properties of uncertainty. Investigating the relationship between patch size and its impact on concept-based explanation quality presents a promising direction for future research.

Additionally, our method for estimating concept importance may not be optimal, as evidenced by the superior performance of using NMF activations directly in our experiments. We suspect this performance gap arises from the variance—or lack thereof—of the uncertainty measure. Specifically, if we perturb a concept within an already highly uncertain input, the uncertainty measure may not exhibit significant variation. While we did not explore alternative ways to refine importance attribution in this study, we do plan to do address it in future iterations of this work.

6 Conclusion

We introduced a novel framework for explaining uncertainty using automatically extracted concept activation vectors. Our proposed framework enables both local and global explanations of uncertainty through the use of importance scores and attribution maps. These explanations demonstrate their utility by being incorporated into rejection strategies, aiding design of useful re-training sets, and helping to detect and mitigate bias. Moreover, while concept-based explanations of model predictions can be useful, using CAVs to capture sources of uncertainty not only offers another complementary view into how a model makes its decisions, but also provides interpretable ways to enhance its performance.

7 Acknowledgements

This project has received funding from the European Union’s Horizon Europe research and innovation programme under the Marie Skłodowska-Curie grant agreement No 101073307.

References

1. Achitbat, R., Dreyer, M., Eisenbraun, I., Bosse, S., Wiegand, T., Samek, W., Lapuschkin, S.: From attribution maps to human-understandable explanations through concept relevance propagation. *Nature Machine Intelligence* **5**(9), 1006–1019 (2023)
2. Antoran, J., Bhatt, U., Adel, T., Weller, A., Hernández-Lobato, J.M.: Getting a {clue}: A method for explaining uncertainty estimates. In: International Conference on Learning Representations (2021)
3. Bitterwolf, J., Müller, M., Hein, M.: In or out? Fixing ImageNet out-of-distribution detection evaluation. In: ICML. vol. 202, pp. 2471–2506 (2023), <https://proceedings.mlr.press/v202/bitterwolf23a.html>
4. Bley, F., Lapuschkin, S., Samek, W., Montavon, G.: Explaining predictive uncertainty by exposing second-order effects. *Pattern Recognition* **160**, 111171 (2025)
5. Burkart, N., Huber, M.F.: A survey on the explainability of supervised machine learning. *Journal of Artificial Intelligence Research* **70**, 245–317 (2021)
6. Daxberger, E., Kristiadi, A., Immer, A., Eschenhagen, R., Bauer, M., Hennig, P.: Laplace redux - effortless bayesian deep learning. In: Ranzato, M., Beygelzimer, A., Dauphin, Y., Liang, P., Vaughan, J.W. (eds.) *Advances in Neural Information Processing Systems*. vol. 34, pp. 20089–20103. Curran Associates, Inc. (2021)
7. De-Arteaga, M., Romanov, A., Wallach, H., Chayes, J., Borgs, C., Chouldechova, A., Geyik, S., Kenthapadi, K., Kalai, A.T.: Bias in bios: A case study of semantic representation bias in a high-stakes setting. In: Proceedings of the Conference on Fairness, Accountability, and Transparency. p. 120–128. FAT* '19, Association for Computing Machinery, New York, NY, USA (2019)
8. Deng, J., Dong, W., Socher, R., Li, L.J., Li, K., Fei-Fei, L.: ImageNet: A Large-Scale Hierarchical Image Database. In: CVPR09 (2009)
9. Depeweg, S., Hernandez-Lobato, J.M., Doshi-Velez, F., Udluft, S.: Decomposition of uncertainty in bayesian deep learning for efficient and risk-sensitive learning. In: International conference on machine learning. pp. 1184–1193. PMLR (2018)
10. Devlin, J., Chang, M.W., Lee, K., Toutanova, K.: BERT: Pre-training of deep bidirectional transformers for language understanding. In: Burstein, J., Doran, C., Solorio, T. (eds.) *Proceedings of the 2019 Conference of the North American Chapter of the Association for Computational Linguistics: Human Language Technologies, Volume 1 (Long and Short Papers)*. pp. 4171–4186. Association for Computational Linguistics, Minneapolis, Minnesota (Jun 2019). <https://doi.org/10.18653/v1/N19-1423>, [https://aclanthology.org/N19-1423/](https://aclanthology.org/N19-1423)
11. Fel, T., Boutin, V., Béthune, L., Cadène, R., Moayeri, M., Andéol, L., Chalvidal, M., Serre, T.: A holistic approach to unifying automatic concept extraction and concept importance estimation. *Advances in Neural Information Processing Systems* **36** (2024)
12. Fel, T., Cadène, R., Chalvidal, M., Cord, M., Vigouroux, D., Serre, T.: Look at the variance! efficient black-box explanations with sobol-based sensitivity analysis. *NeurIPS* **34**, 26005–26014 (2021)
13. Fel, T., Picard, A., Bethune, L., Boissin, T., Vigouroux, D., Colin, J., Cadène, R., Serre, T.: Craft: Concept recursive activation factorization for explainability. In: Proceedings of the IEEE/CVF Conference on Computer Vision and Pattern Recognition. pp. 2711–2721 (2023)
14. Gal, Y., Ghahramani, Z.: Dropout as a bayesian approximation: Representing model uncertainty in deep learning. In: international conference on machine learning. pp. 1050–1059. PMLR (2016)

15. Gawlikowski, J., Tassi, C.R.N., Ali, M., Lee, J., Humt, M., Feng, J., Kruspe, A., Triebel, R., Jung, P., Roscher, R., et al.: A survey of uncertainty in deep neural networks. *Artificial Intelligence Review* **56**(Suppl 1), 1513–1589 (2023)
16. Ghorbani, A., Wexler, J., Zou, J.Y., Kim, B.: Towards automatic concept-based explanations. In: Wallach, H., Larochelle, H., Beygelzimer, A., d'Alché-Buc, F., Fox, E., Garnett, R. (eds.) *Advances in Neural Information Processing Systems*. vol. 32. Curran Associates, Inc. (2019)
17. Hendrickx, K., Perini, L., Van der Plas, D., Meert, W., Davis, J.: Machine learning with a reject option: A survey. *Machine Learning* **113**(5), 3073–3110 (2024)
18. Jourdan, F., Picard, A., Fel, T., Risser, L., Loubes, J.M., Asher, N.: COCKATIEL: COntinuous concept ranKed ATtribution with interpretable ELeMents for explaining neural net classifiers on NLP. In: Rogers, A., Boyd-Graber, J., Okazaki, N. (eds.) *Findings of the Association for Computational Linguistics: ACL 2023*. pp. 5120–5136. Association for Computational Linguistics, Toronto, Canada (Jul 2023)
19. Kim, B., Wattenberg, M., Gilmer, J., Cai, C., Wexler, J., Viegas, F., Sayres, R.: Interpretability beyond feature attribution: Quantitative testing with concept activation vectors (tcav) (2018), <https://arxiv.org/abs/1711.11279>
20. Kirsch, A., Van Amersfoort, J., Gal, Y.: Batchbald: Efficient and diverse batch acquisition for deep bayesian active learning. *Advances in neural information processing systems* **32** (2019)
21. Lakshminarayanan, B., Pritzel, A., Blundell, C.: Simple and scalable predictive uncertainty estimation using deep ensembles. *Advances in neural information processing systems* **30** (2017)
22. Marx, C., Park, Y., Hasson, H., Wang, Y., Ermon, S., Huan, L.: But are you sure? an uncertainty-aware perspective on explainable ai. In: *International Conference on Artificial Intelligence and Statistics*. pp. 7375–7391. PMLR (2023)
23. Nadeem, M.S.A., Zucker, J.D., Hanczar, B.: Accuracy-rejection curves (arcs) for comparing classification methods with a reject option. In: Džeroski, S., Guerts, P., Rousu, J. (eds.) *Proceedings of the third International Workshop on Machine Learning in Systems Biology. Proceedings of Machine Learning Research*, vol. 8, pp. 65–81. PMLR, Ljubljana, Slovenia (05–06 Sep 2009), <https://proceedings.mlr.press/v8/nadeem10a.html>
24. Osband, I., Blundell, C., Pritzel, A., Van Roy, B.: Deep exploration via bootstrapped dqn. *Advances in neural information processing systems* **29** (2016)
25. Shaker, M.H., Hüllermeier, E.: Aleatoric and epistemic uncertainty with random forests. In: Berthold, M.R., Feelders, A., Kreml, G. (eds.) *Advances in Intelligent Data Analysis XVIII*. pp. 444–456. Springer International Publishing, Cham (2020)
26. Smith, L., Gal, Y.: Understanding measures of uncertainty for adversarial example detection. In: Globerson, A., Silva, R. (eds.) *Proceedings of the Thirty-Fourth Conference on Uncertainty in Artificial Intelligence, UAI 2018, Monterey, California, USA, August 6-10, 2018*. pp. 560–569. AUAI Press (2018)
27. Wang, H., Joshi, D., Wang, S., Ji, Q.: Gradient-based uncertainty attribution for explainable bayesian deep learning. In: *Proceedings of the IEEE/CVF Conference on Computer Vision and Pattern Recognition*. pp. 12044–12053 (2023)
28. Watson, D., O'Hara, J., Tax, N., Mudd, R., Guy, I.: Explaining predictive uncertainty with information theoretic shapley values. *Advances in Neural Information Processing Systems* **36** (2024)

8 Appendix

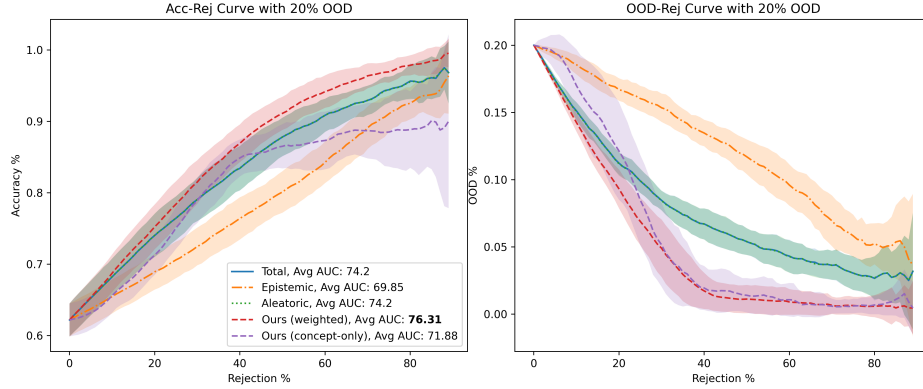


Figure 6: (left) Accuracy-Rejection (\uparrow) and (right) OOD-Rejection Curves (\downarrow) with 20% OOD data.

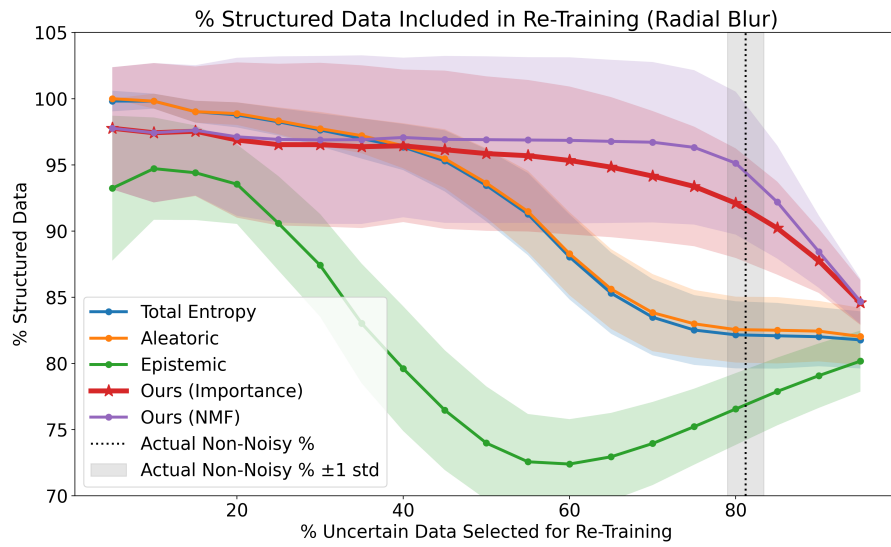


Figure 7: (left) Radial Blur experiment results (\uparrow).

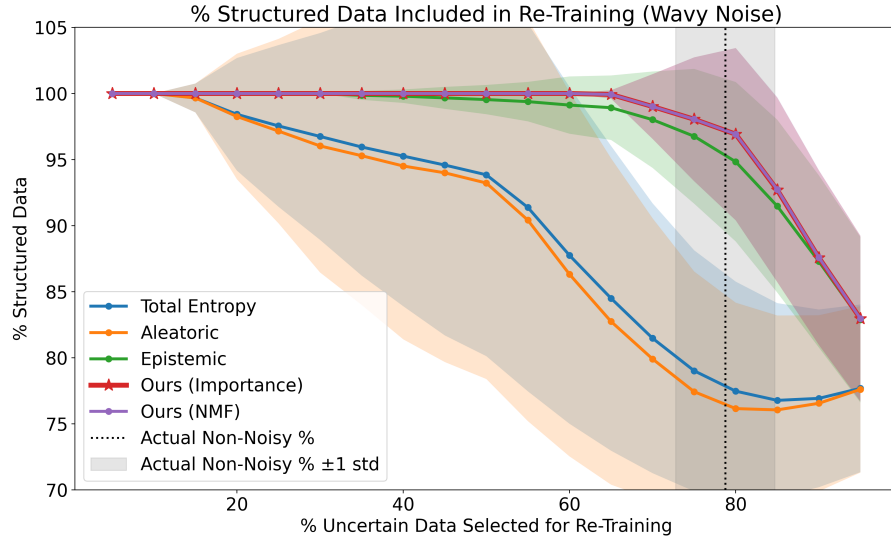


Figure 8: (left) Wave Noise experiment results (↑).

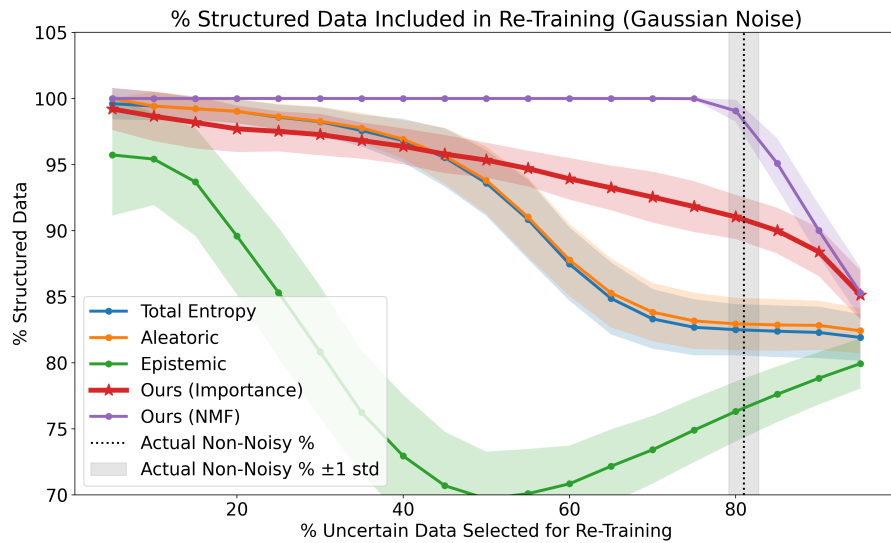


Figure 9: (left) Radial Blur experiment results (↑).

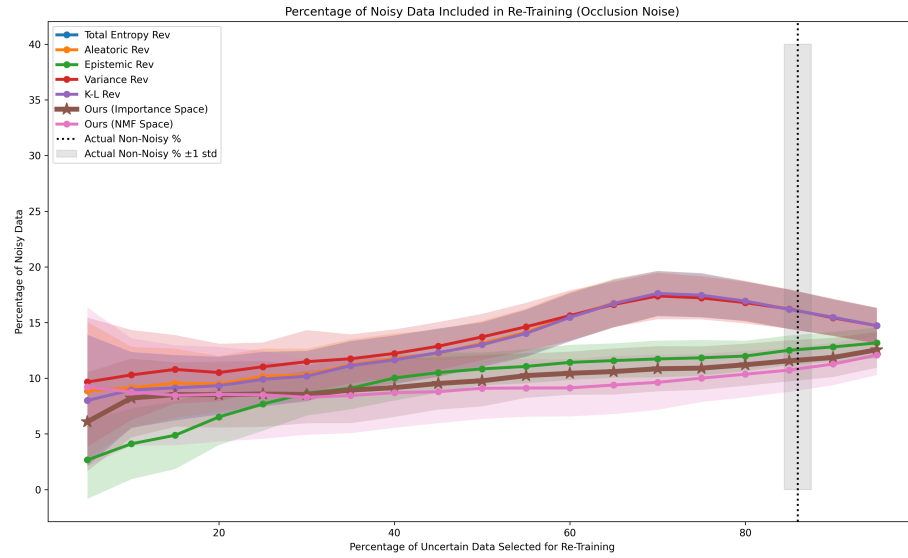


Figure 10: (left) Occlusion experiment results (\uparrow) and an example noisy image (right).

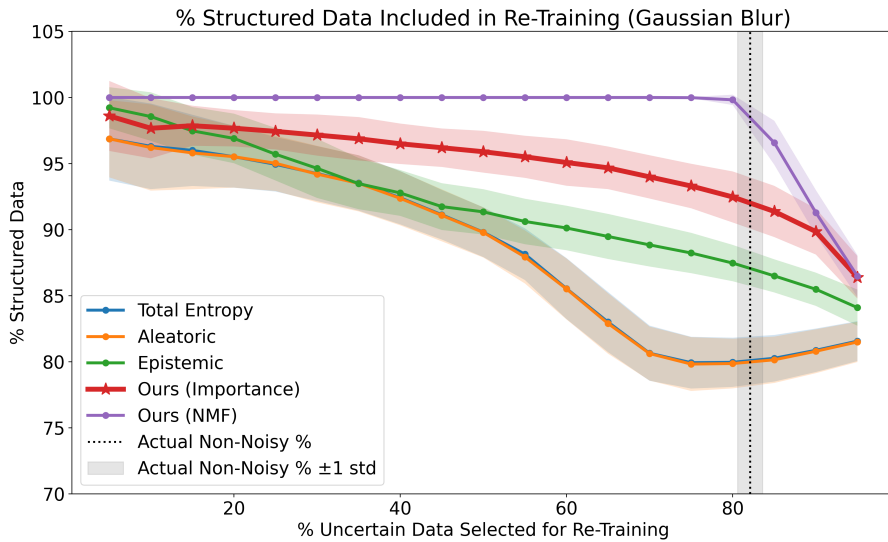
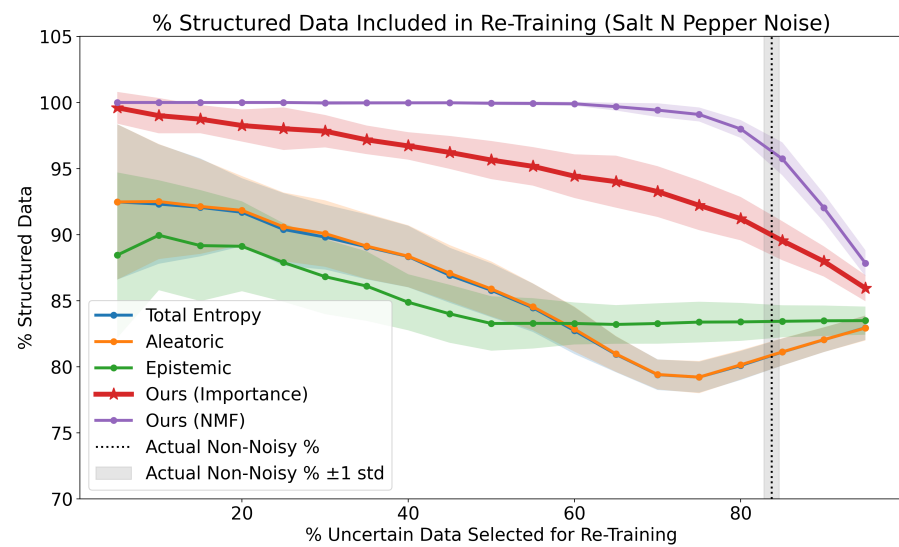


Figure 11: (left) Gaussian Blur experiment results (\uparrow).

Figure 12: (left) Salt and Pepper noise experiment results (\uparrow).